Farrag *et al. Behavioral and Brain Functions (2024) 20:26*
https://doi.org/10.1186/s12993-024-00250-1

Behavioral and
Brain Functions

RESEARCH

Open Access

Comparative effect of atorvastatin and risperidone on modulation of TLR4/NF-κB/NOX-2 in a rat model of valproic acid-induced autism

Eman A. E. Farrag[1*], Mona H. Askar[2], Zienab Abdallah[2], Safinaz M. Mahmoud[3], Eman A. Abdulhai[4], Eman Abdelrazik[5], Eman Mohamad El Nashar[6], Faten Mohammed Alasiri[7], Asma Nasser Saeed Alqahtani[8], Mamdouh Eldesoqui[9,10], Ali M. Eldib[11,12] and Alshimaa Magdy[13]

Abstract

Background Autism spectrum disorder (ASD) is a complex neurodevelopmental condition that is significantly increasing, resulting in severe distress. The approved treatment for ASD only partially improves the sympoms, but it does not entirely reverse the symptoms. Developing novel disease-modifying drugs is essential for the continuous improvement of ASD. Because of its pleiotropic effect, atorvastatin has been garnered attention for treating neuronal degeneration. The present study aimed to investigate the therapeutic effects of atorvastatin in autism and compare it with an approved autism drug (risperidone) through the impact of these drugs on TLR4/NF-κB/NOX-2 and the apoptotic pathway in a valproic acid (VPA) induced rat model of autism.

Methods On gestational day 12.5, pregnant rats received a single IP injection of VPA (500 mg/kg), for VPA induced autism, risperidone and atorvastatin groups, or saline for control normal group. At postnatal day 21, male offsprings were randomly divided into four groups (n = 6): control, VPA induced autism, risperidone, and atorvastatin. Risperidone and atorvastatin were administered from postnatal day 21 to day 51. The study evaluated autism-like behaviors using the three-chamber test, the dark light test, and the open field test at the end of the study. Biochemical analysis of TLR4, NF-κB, NOX-2, and ROS using ELISA, RT-PCR, WB, histological examination with hematoxylin and eosin and immunohistochemical study of CAS-3 were performed.

Results Male offspring of prenatal VPA-exposed female rats exhibited significant autism-like behaviors and elevated TLR4, NF-κB, NOX-2, ROS, and caspase-3 expression. Histological analysis revealed structural alterations. Both risperidone and atorvastatin effectively mitigated the behavioral, biochemical, and structural changes associated with VPA-induced rat model of autism. Notably, atorvastatin group showed a more significant improvement than risperidone group.

Conclusions The research results unequivocally demonstrated that atorvastatin can modulate VPA-induced autism by suppressing inflammation, oxidative stress, and apoptosis through TLR4/NF-κB/NOX-2 signaling pathway. Atorvastatin could be a potential treatment for ASD.

Keywords Valproic acid, Autism, Atorvastatin, Risperidone, TLR4, NF-κB, Apoptosis

*Correspondence:
Eman A. E. Farrag
dreman_abdo_2010@mans.edu.eg
Full list of author information is available at the end of the article

Graphical Abstract

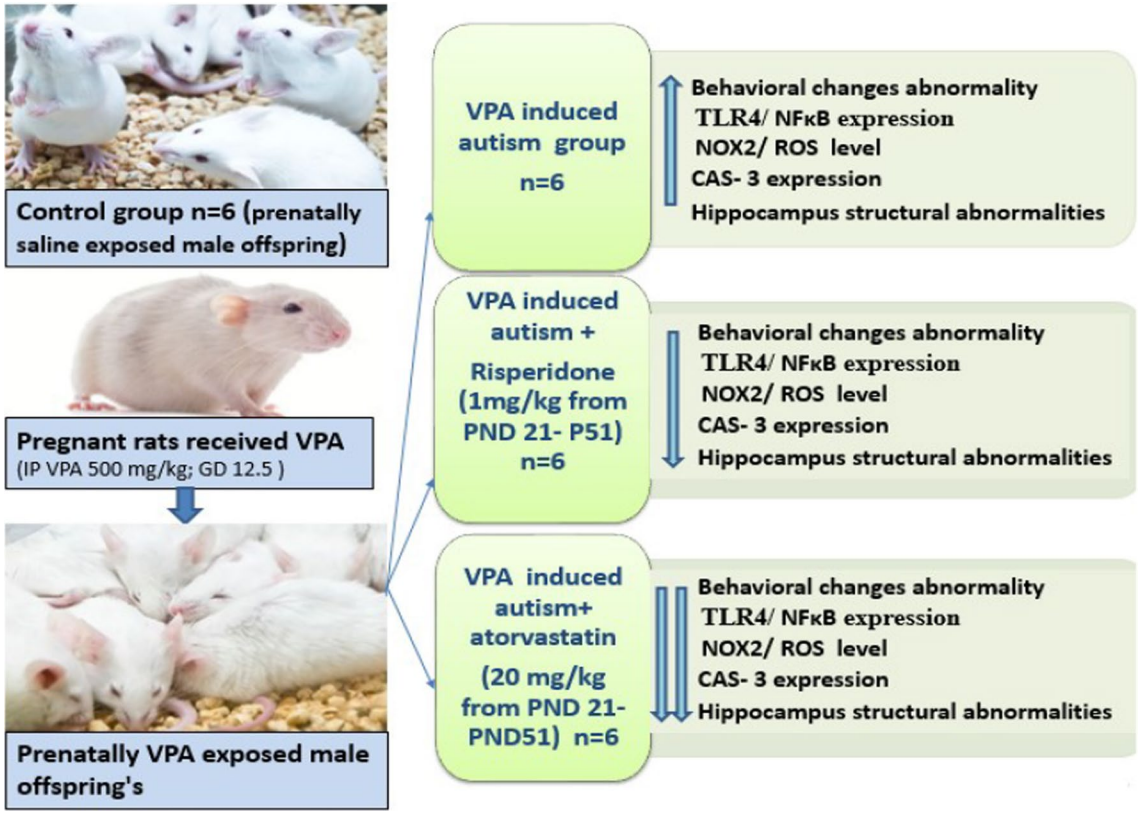

Introduction

Autism spectrum disorder (ASD) is a complicated neurodevelopmental disease that manifests as altrered social interaction, behaviors, and limited interests [1]. SD is usually noticeable in the first three years of life and continues into adulthood in most cases [2]. According to Ebrahimi et al., the prevalence of ASD is 1 in 54 individuals. In males, the prevalence is four times greater [3].

Despite all efforts to clarify ASD, its pathological mechanisms are still unidentified, and the disease has reached epidemic levels, making it a vastly distressing disease [4]. Altered immune function and regulation have been emphasized in the pathogenesis of ASD [3]. Toll-like receptor (TLR) signaling significantly controls both innate and adaptive immunity [5], and plays a significant role in the neuroinflammatory progression in ASD mouse models [6]. TLR-4 is the leading cause of ASD because it activates inflammatory cytokines and reactive oxygen species (ROS) [7, 8].

The nuclear factor kappa-light-chain enhancer of activated B cells (NF-κB) pathway is activated by TLR-4 signaling [8, 9]. Children with autism have higher levels of TLR-4 and NF-κB, accompanied by increased nicotinamide adenine dinucleotide phosphate (NADPH) oxidase 2 (NOX2) and ROS signaling [2]. Extra ROS at the cellular level damages nucleic acids, proteins, lipids, membranes, and organelles, resulting in apoptosis [10]. ROS signals stimulate the production of inflammatory genes and prompt apoptosis [11]. An external or internal pathway that triggers apoptosis eventually activates caspase-3 (CAS-3), a crucial factor in programmed cell death [12, 13].

As a result, the pathogenesis of ASD remains a subject of speculation; effective treatments for ASD are unattainable to date [14]. Risperidone, a second-generation antipsychotic, alleviates anxity and rapid mood swings. Studies have reported a significant alleviation in symptoms linked to autism [15]. Only risperidone and aripiprazole have been appoved by Food and Drug Administration (FDA) for disruptive ASD treatment; however, these drugs only recover some sympotoms and do not fully reverse ASD features. The lifelong social and economic burdens of ASD necessitate continuous, active study for effective treatment [16]. Developing

novel autism disease-modifying neuroprotective drugs is essential for the continuous improvement of ASD features [17]. Neuroprotection preventing cell death, restoring neuronal numbers and behavioral output [18].

Our study, a continuation of research on the development of effective neuroprotective drugs for autism, focused on the role of atorvastatin in the VPA-induced autism rat model. Statins are 3-hydroxy-3-methylglutaryl coenzyme A (HMG-CoA) reductase inhibitors. In addition to their primarily defined lipid-depressing effects, they have pleiotropic effects, including anti-inflammatory, antioxidant, and other effects [19]. Statins may have therapeutic uses against numerous diseases, including autoimmune disorders, dementia, multiple sclerosis, arthritis, and some types of cancer [20].

Atorvastatin is a widely used lipid-lowering medication among statins, and we selected it as a sample statin. Furthermore, multiple previous experimental studies have assessed the neuroprotective efficacy of atorvastatin in an experimental nerve crush injury model [21], against subarachnoid hemorrhage [22]. Additionally, atorvastatin has been shown to aid in the recovery of cognitive function after global cerebral ischemia in rats [23] and inhibit neuronal apoptosis in hypoxic-ischemic neonatal rats [24]. Atorvastatin has anti-inflammatory and antioxidant properties. It suppresses TLR4 gene transcription and protein levels, and reduces inflammatory and oxidative mediators [25]. TLR functions in the neuroinflammatory response in mouse models of ASD [6]. Thus, the current study aimed to estimate the therapeutic effects of atorvastatin and compare them with those in risperidone by examining the role of both drugs in the TLR4/ NF-κB/ NOX2 molecular pathway and apoptosis in a rat model of VPA-induced autism.

Results

Effect of postnatal risperidone/atorvastatin treatment on ASD behavioral changes of prenatally VPA exposed male offspring

Three chamber test

VPA-induced autism offspring exhibited significantly decreased latency compared with the control group. Risperidone- and atorvastatin-treated groups showed a significant increase in latency compared with the untreated VPA-induced autism group. There was a notable escalation in the latency in the atorvastatin group compared with the risperidone-treated group. F value: 54 (Fig. 1, Table 1).

Rat sociability was assessed using three chamber tests. Regarding the time spent in the non-social stimulus (wooden block) zone and the number of entries, the VPA-induced autism group showed significantly increased time and number of entries to this zone compared with the control group. The risperidone and atorvastatin-treated groups showed considerably decreased time and number of entries compared with the VPA-induced autism group. There was a significant decline in the time and number of wooden block zone entries in the atorvastatin group compared with the risperidone group. F values: 26.249 and 48.970 for the time spent in the wooden block zone and the number of entries, respectively.

The VPA-induced autism group showed a significant decrease in the time spent with social stimuli; novel-matched rat, and the number of entries in this zone compared with the control group. The risperidone- and atorvastatin-treated groups showed significant recovery and increased duration spent in the stranger zone compared with the VPA-induced autism group. F values: 24.506 and 29.493 for the time spent in the novel-matched rat zone and the number of entries, respectively (Fig. 1, Table 1).

Dark light test

The light/dark test was reliable for anxiety detection, where VPA-induced autism offspring showed obvious distress in the illuminated area and spent considerably less time in light than normal rats.

Improvement in anxiety in the risperidone- and atorvastatin-treated groups was observed with higher duration spent in the bright partition. Concerning the number of transitions between the light and dark compartments, VPA-induced autism offspring showed significantly increased transitions between the dark and light chambers, which recovered to control levels in both the atorvastatin and risperidone groups. More transitions also confirmed a high level of anxiety, which was detected in prenatal VPA induced autism, and a significant decrease in both risperidone- and atorvastatin-treated groups. F values: 56.241 and 28.302 for duration in the light chamber and the number of transitions, respectively (Fig. 2, Table 1).

Open field test

Motor performance and hyperactivity were evaluated by the distance traveled and the number of attempts to go to the center in the open field test. In addition, anxiety was determined in this test by evaluating the stretched attended posture. There was an increase in hyperactivity and stress in the VPA-induced autism group, which were alleviated by risperidone and atorvastatin treatment; there were statistically significant increases in the distance moved, number of attempts to go to the center, and stretched attended posture in the VPA-induced autism group compared with the control group. Both risperidone and atorvastatin-treated groups showed significant decreases in distance moved, the number of times they

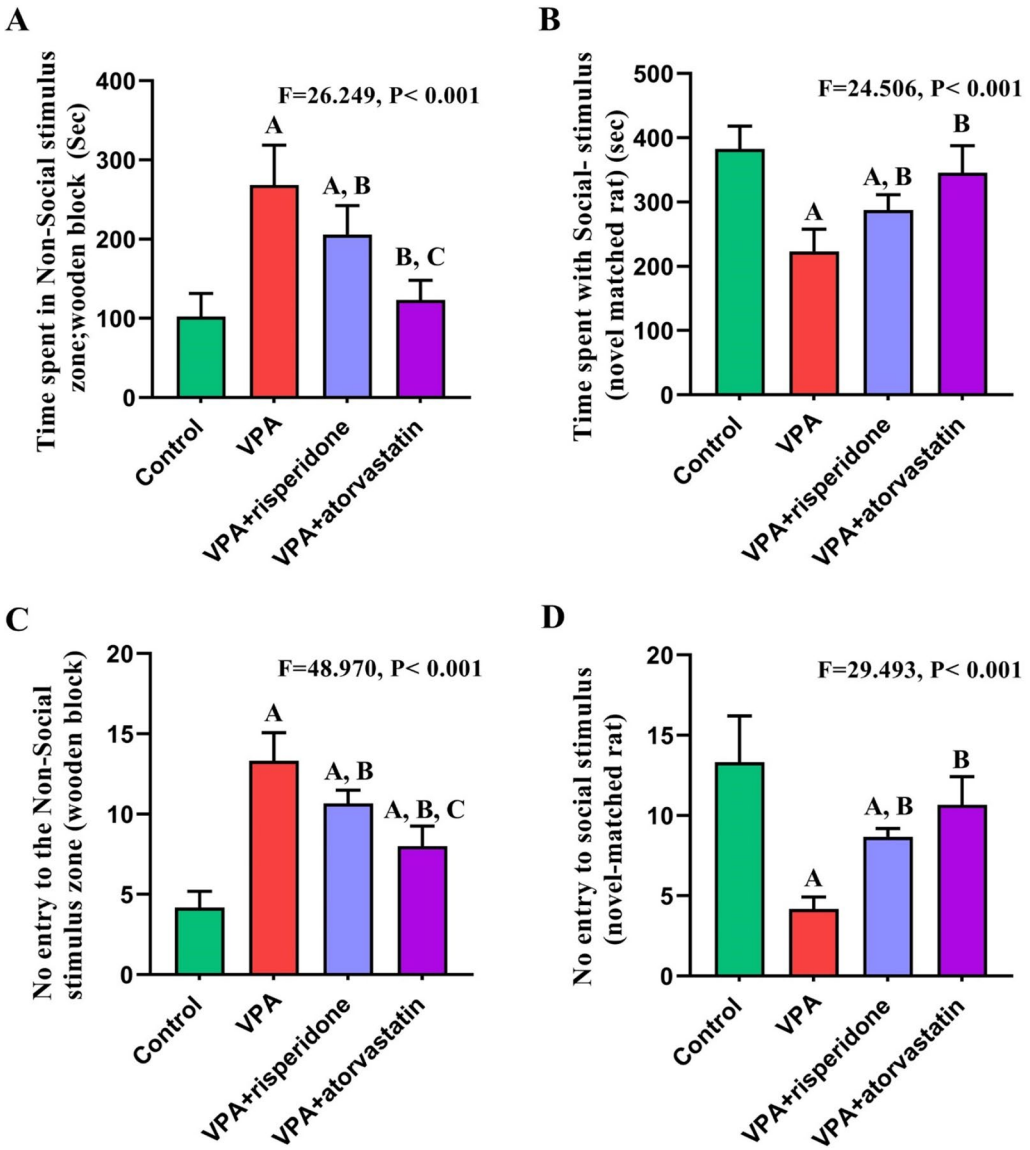

Fig. 1 Effect of risperidone/atorvastatin treatment on the three-chamber test (time spent in non-social and social stimulus **A**, **B** number of enteries to non-social and social stimulus **C**, **D**) in prenatally VPA-exposed male offspring. Data are expressed as mean ± SD. One-way ANOVA and the post-hoc Tukey's tests were used to compare between groups. P value ≤ 0.05 is significant. **A**, **B**, and **C** represent significance for the control, VPA, and VPA + risperidone groups, respectively. (P value < 0.001). VPA: valproic acid

went to the center, and stretched attended posture compared with the untreated VPA-induced autism group. F value: 33.428, 14.959,32.604 for the distance moved, the number went to the center and stretched attended posture respectively (Fig. 2, Table 1).

Effect of postnatal risperidone/atorvastatin treatment on TLR4 levels in the hippocampi of prenatally VPA-exposed male offspring

To elucidate the role of the TLR4 molecular pathway in the pathogenesis of ASD and the effects of risperidone and atorvastatin treatment, TLR4 gene expression, reverse transcription polymerase chain reaction (RT-PCR), protein expression (Western blot) were assessed. The VPA-induced autism group exhibited a notable increases in TLR4 gene expression and protein level. Treatment with risperidone or atorvastatin significantly reduced TLR4 gene expression and protein level compared with the VPA-induced autism group. Atorvastatin distinctly reduces TLR4 expression compared with risperidone administration. F values: 81.882 and 144.050 for RT-PCR and western blot, respectively (Fig. 3).

Table 1 Data are expressed as mean ± SD

Parameters	Study groups				F value	P value
	Control group (n = 6)	VPA-induced autism group (n = 6)	VPA + risperidone group (n = 6)	VPA + atorvastatin group (n = 6)		
Three chamber test						
Latency	12.50 ± 1.87	3.50 ± 1.05 *	8.17 ± .98 *&	10.50 ± 1.05 &#	54	< 0.001
Time spent in Non-Social stimulus zone (wooden block) (sec)	102.33 ± 29.30	268.50 ± 50.41 *	205.67 ± 36.86 *&	123 ± 25.03 &#	26.249	< 0.001
Number of entry to the Non-Social stimulus zone (wooden block)	4.17 ± 1.02	13.33 ± 1.75 *	10.67 ± 0.82 *&	8 ± 1.26 &#	48.970	< 0.001
Time spent with Social- stimulus (novel matched rat) (sec)	382.67 ± 35.52	223.17 ± 34.49 *	287.50 ± 23.86 *&	345.83 ± 41.82 &#	24.506	< 0.001
Number of entry to Social stimulus (novel-matched rat)	13.33 ± 2.88	4.17 ± 0.75 *	8.67 ± 0.52 *&	10.67 ± 1.75 &	29.493	< 0.001
Dark light test						
The duration in the light chamber (Sec)	485.83 ± 33.90	240.83 ± 50.25 *	389.50 ± 33.82 *&	464.83 ± 20.85 &#	56.241	< 0.001
Number of transitions	13.67 ± 3.27	31.50 ± 4.93 *	22.50 ± 3.2 7 *&	17.50 ± 2.17 &	28.302	< 0.001
Open field test						
Distance moved (No. of squares)	57.50 ± 18.23	183.33 ± 36.65 *	110.67 ± 21.86 *&	73.67 ± 9.79 &	33.428	< 0.001
Number of goes to center	4.60 ± 1.52	12.83 ± 2.79 *	9.67 ± 2.66 *&	6.50 ± 2.07 &	14.959	< 0.001
Stretched attended posture	19.33 ± 2.88	37 ± 3.58 *	27.67 ± 2.42 *&	23 ± 4 &	32.604	< 0.001

VPA, valproic acid

One-way ANOVA test and post hoc Tukey's test were used to compare the groups

* significance with the control group,

& significance with VPA induced autism group

significance with risperidone treated group

P value ≤ 0.05 is significant

Effect of postnatal risperidone/atorvastatin treatment on NF-κB level in the hippocampi of prenatally VPA-exposed male offspring

The VPA-induced autism group showed increased NF-κB expression by RT-PCR, and protein level by Enzyme-Linked Immunosorbent Assay (ELISA), compared with the control group. Treatment with either risperidone or atorvastatin remarkably declined NF-κB levels compared with the VPA-induced autism group. The atorvastatin-treated group showed significantly reduced NF-κB levels in the hippocampus compared with the risperidone-treated group. F values: 110.652 and 171. 820 for RT-PCR and ELISA, respectively (Fig. 4).

Effect of postnatal risperidone/atorvastatin treatment on NOX2/total ROS markers in the hippocampi of prenatally VPA exposed male offspring

The VPA-induced autism group showed a notable escalation in NOX2 expression and protein levels compared with the control group. Treatment with either risperidone or atorvastatin markedly reduced this level compared with that in the VPA-induced autism group. Furthermore, the atorvastatin-treated group showed significantly reduced NOX2 levels in the hippocampus compared with the risperidone group F values: 110. 652, 157. 995 for RT-PCR and ELISA, respectively (Fig. 5).

Regarding total ROS, VPA induced autism group exhibited a highly significant increase in ROS levels compared with the control group. Treatment with risperidone or atorvastatin appreciably decreased the total ROS level compared with the VPA-induced autism group. In addition, total ROS levels were significantly decreased in atorvastatin group compared with the risperidone group. F value: 115. 578 (Fig. 5).

Effect of postnatal risperidone/atorvastatin treatment on the hippocampal histopathology of prenatally VPA exposed male offsprings

Hematoxylin and eosin (H&E) stain

The hippocampal formation mainly comprises the hippocampus proper and dentate gyrus (Fig. 6A). The Cornu Ammonis 3 (CA3) area of the hippocampus of the control rats contains large pyramidal cells with large vesicular nuclei in the pyramidal layer. Both the molecular and polymorphic layers contained few glial cells, neuronal processes, and scattered nerve cells (Fig. 6B). The CA3

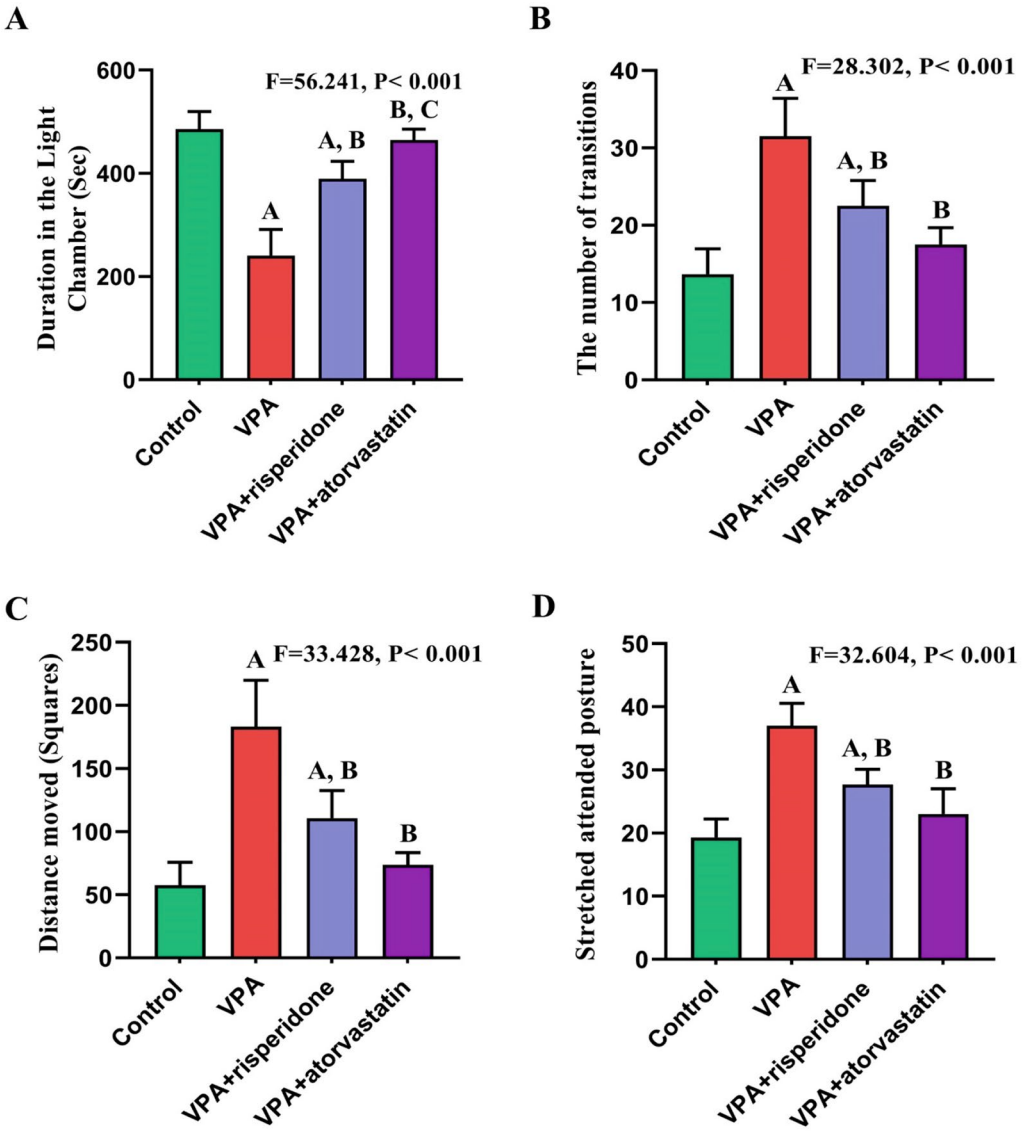

Fig. 2 Effect of risperidone/ atorvastatin treatment on the dark light test; duration in the light chamber and number of transitions (**A**, **B**) and open field tests; distance traveled and stretched attended posture (**C**, **D**) tests in prenatally VPA-exposed male offspring. Data are expressed as mean ± SD. One-way ANOVA test and the post hoc Tukey's tests were used to compare groups and P value ≤ 0.05 is significant. **A**, **B**, and **C** represent significance for the control, VPA, and risperidone groups, respectively. (P value < 0.001). VPA: valproic acid

region of the VPA-induced autism group revealed small shrunken pyramidal cells with darkly stained cytoplasm and pyknotic nuclei. Areas devoid of cells can be seen leaving wide intercellular spaces (Fig. 6C).

The CA3 region of the risperidone-treated group showed that most of pyramidal cells appeared normal with large vesicular nuclei, apart from some shrunken cells with darkly stained cytoplasm and pyknotic nuclei. Blood vessels were seen (Fig. 6D). The CA3 region of the atorvastatin-treated group showed that most pyramidal cells were normal with large vesicular nuclei, and only a limited number of shrunken cells appeared with darkly stained cytoplasm and pyknotic nuclei (Fig. 6E).

Immunohistochemical

TLR4 immunostaining Immunostaining with anti-TLR4 antibody in the hippocampus of the control group exhibited an adverse immune reaction (Fig. 7A). In contrast, the VPA-induced autism group exhibited numerous cells with a solid positive immune reaction as a brown cytoplasmic color (Fig. 7B). The risperidone- and atorvastatin-treated groups showed only a few cells with positive

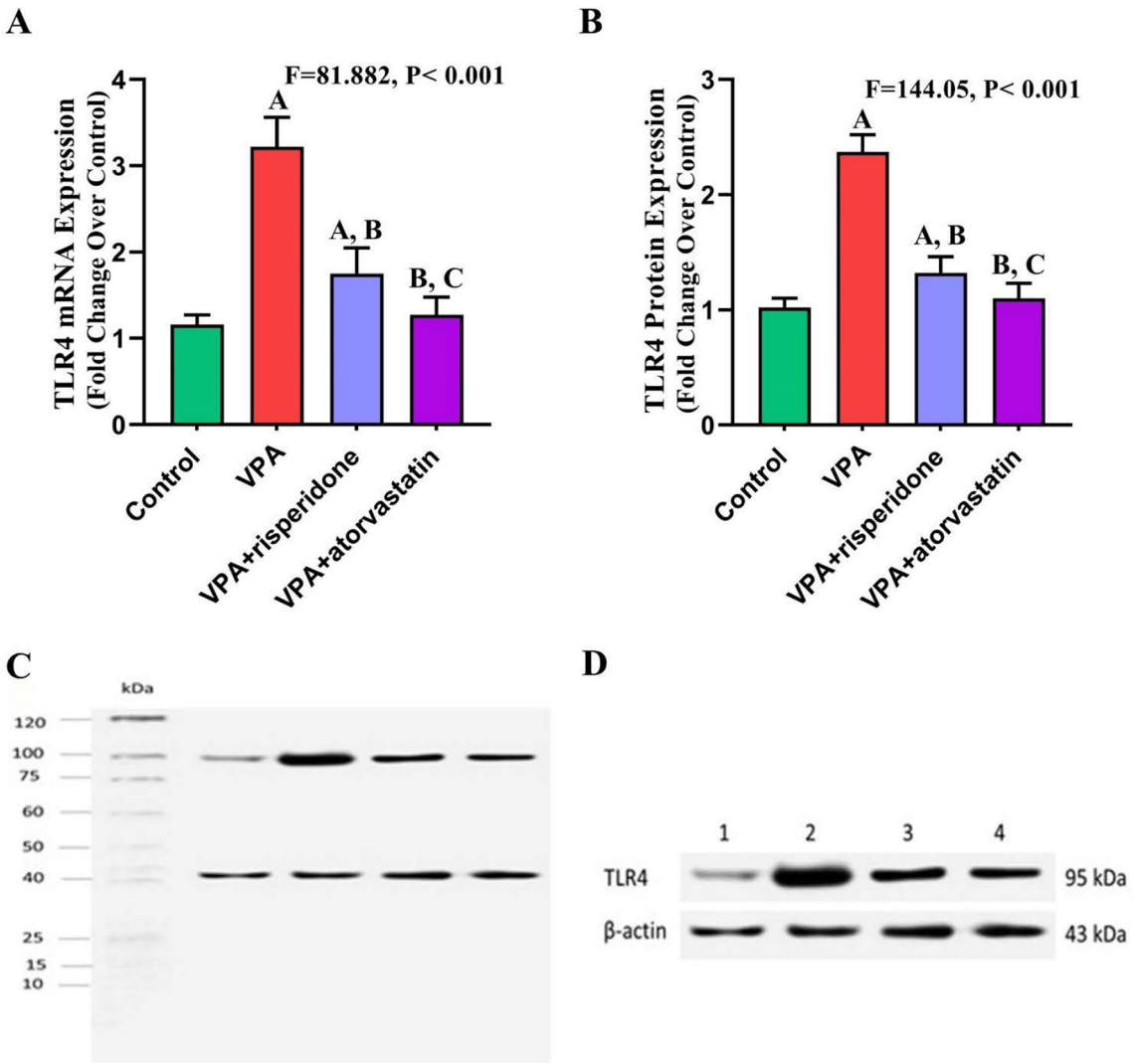

Fig. 3 Effect of risperidone/atorvastatin treatment on the TLR4 marker in the hippocampi of prenatally VPA-exposed male offspring. **A** TLR4 mRNA expression as detected by RT-PCR. **B** TLR4 protein relative quantitation by WB. **C** Representative picture for uncropped blot (whole ladder) including TLR4, β actin protein expression by western blot. **D** Cropped blot of TLR4, β-actin protein bands with their molecular weight (molecular weight: 95, 43 kDa, respectively). β-actin is selected as an endogenous control. Data are expressed as mean ± SD. One-way ANOVA test and the post hoc Tukey's tests were used to compare groups, **A**, **B**, and **C** represent significance for the control, VPA, and risperidone groups, respectively. P value ≤ 0.05 is significant (P values significance with control, VPA, VPA + risperidone group respectively are: RT-PCR; 0.001, 0.001, 0.019. WB; 0.001, 0.001, 0.027). VPA: valproic acid. TLR4, toll-like receptor 4

immune responses, whereas most had an adverse immune reaction (Fig. 7C, D).

Statistical analysis of the number of TLR4-positive immune cells in the CA3 region denoted a highly significant increase in the number of positive cells in the VPA-induced autism group compared with the control group. In the risperidone-treated group, the number of positive cells exhibited a notable decline compared with the VPA-induced autism group and a remarkable rise compared with the control group. Likewise, positive cell numbers in the atorvastatin-treated group revealed a significant reduction compared with the VPA-induced autism group but without significant change compared with the control and risperidone-treated groups. F value: 37.615 (Fig. 7E).

Caspase 3 (CAS-3) immunostaining Immunostaining with anti-caspase 3 antibodies of the hippocampus of the control group exhibited a negative immune reaction (Fig. 8A), whereas, in the VPA-induced autism group, a solid positive immune reaction was identified as a brown color in the cytoplasm of most pyramidal cells (Fig. 8B). The risperidone and atorvastatin-treated groups exhib-

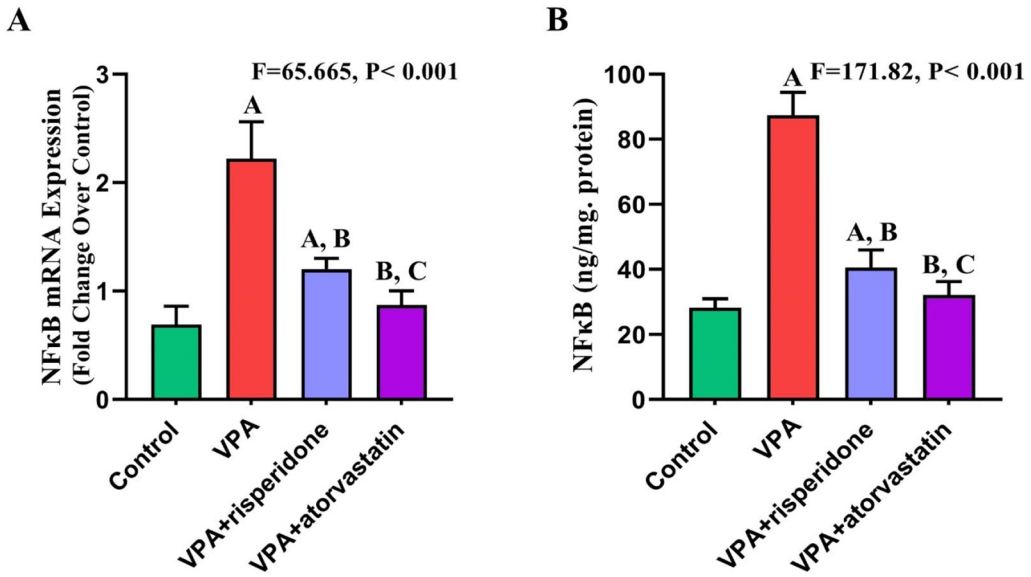

Fig. 4 Effect of risperidone/atorvastatin treatment on NFKβ marker in the hippocampi of prenatally VPA-exposed male offspring. **A** NFκB mRNA expression as detected by RT-PCR. **B** NFκB protein level as detected by ELISA. Data are expressed as mean ± SD. One-way ANOVA and post hoc Tukey's tests were used to compare the groups. **A**, **B**, and **C** represent significance for the control, VPA, and risperidone groups, respectively. P value ≤ 0.05 is significant (P values significance with control, VPA, VPA + risperidone group respectively are: RT-qPCR; 0.001, 0.001, 0.049. ELISA; 0.001, 0.001, 0.042). VPA: valproic acid. NFκβ; nuclear factor kappa

ited only a few cells with positive immune reactions, whereas most cells exhibited a negative immune reaction (Fig. 8C, D).

Statistical analysis of the number of CAS-3-positive immune cells in the CA3 region showed a notable increase in the number of positive cells in the VPA-exposed group compared with the control group. In the risperidone-treated group, the number of positive cells exhibited a noteworthy reduction compared with the VPA-induced autism group and a significant increase compared with the control group. Also, the number of positive cells in the atorvastatin-treated group was significantly lower than in the VPA-induced autism group. However, there was no significant change in the number of positive cells in the control or risperidone-treated groups. F value: 84.244 (Fig. 8E).

Discussion

With the increasing incidence of ASD, care costs are expected to increase reliably over the next decade. The approved ASD treatment remains focused on symptom alleviation. Therefore, neuroprotective agents should be considered a priority for treating ASD through its pathogenic mechanisms [26]. Neuroprotective agents should be able to restore neural regeneration and maintain normal cellular function and behavior [18]. Atorvastatin has gained increasing attention because of its anti-inflammatory, anti-oxidative, anti-apoptotic, and lipid-lowering effects [27]. Thus, this study demonstrated the impact of atorvastatin on ASD compared with risperidone.

Rats exposed to VPA prenatally have been shown to exhibit behavioral changes related to human ASD [28–31]. GD 12.5 is the acclaimed period for the VPA induced autism in rats [32]. The 12th to 13th days of GD are critical periods for neuronal development. Therefore, male offspring exposed to VPA on GD 12.5 showed behaviors, biochemical profiles, and neuroanatomical traits similar to those observed in autism-induced patients [33]. In our study, VPA neurotoxic exposure at a dose of (500 mg/kg) in GD 12.5 provoked ASD behavioral defects in male offspring. VPA-exposed rats showed reduced sociability (a lower favorite for novel rats), raised anxiety levels (increased escaping of the illuminated compartment and stretched attended posture), and hyperactivity (increased distance traveled and the number of times they went to the center in the open field test). Decreased sociability, anxiety, and hyperactivity in rats matched with autism patients [34, 35].

The three-chamber social test was used to evaluate impaired sociability. VPA exposure prenatally revealed a significant reduction in sociability. Social dysfunction in a rat model of VPA-induced autism is expected to result from impairmed cognitive functions [36]. Compared with the VPA-induced autism group, the risperidone- and atorvastatin-treated groups showed significant social improvement, whereas the significance was higher in the

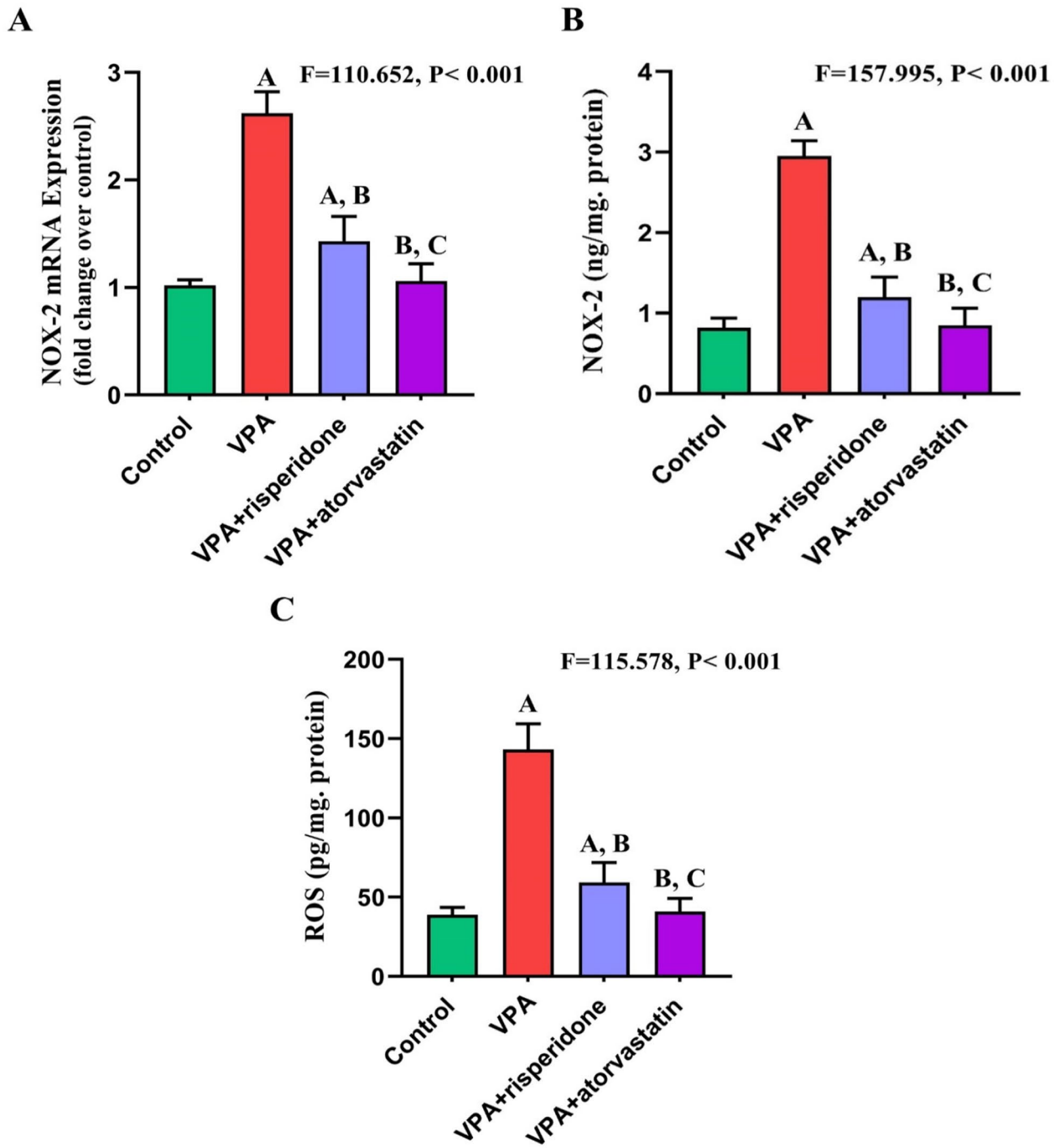

Fig. 5 Effect of risperidone/atorvastatin treatment on NOX2/ ROS markers in the hippocampi of prenatally VPA-exposed male offspring. **A** *NOX2* mRNA expression as detected by RT-qPCR. **B** *NOX2* protein level determined by ELISA. **C** Total ROS as determined by ELISA. Data are expressed as mean ± SD. One-way ANOVA and post hoc Tukey's tests were used to compare the groups. **A**, **B**, and **C** represent significance for the control, VPA, and risperidone groups, respectively. P value ≤ 0.05 is significant (P values significance with control, VPA, VPA + risperidone group respectively are: NOX2 RT-qPCR; 0.001, 0.001, 0.007. NOX2 ELISA; 0.001, 0.001, 0.028. total ROS ELISA; 0.001, 0.001, 0.046)VPA; valproic acid. NOX2; NADPH oxidase. ROS, reactive oxygen species

atorvastatin-treated group. The enhanced sociability of rats treated with either risperidone or atorvastatin was reported in previous studies [37–39].

Anxiety is considered a vital comorbidity in ASD, and approximately 40% of autistic children have standards for an anxiety diagnosis [40]. The light-dark switch test is

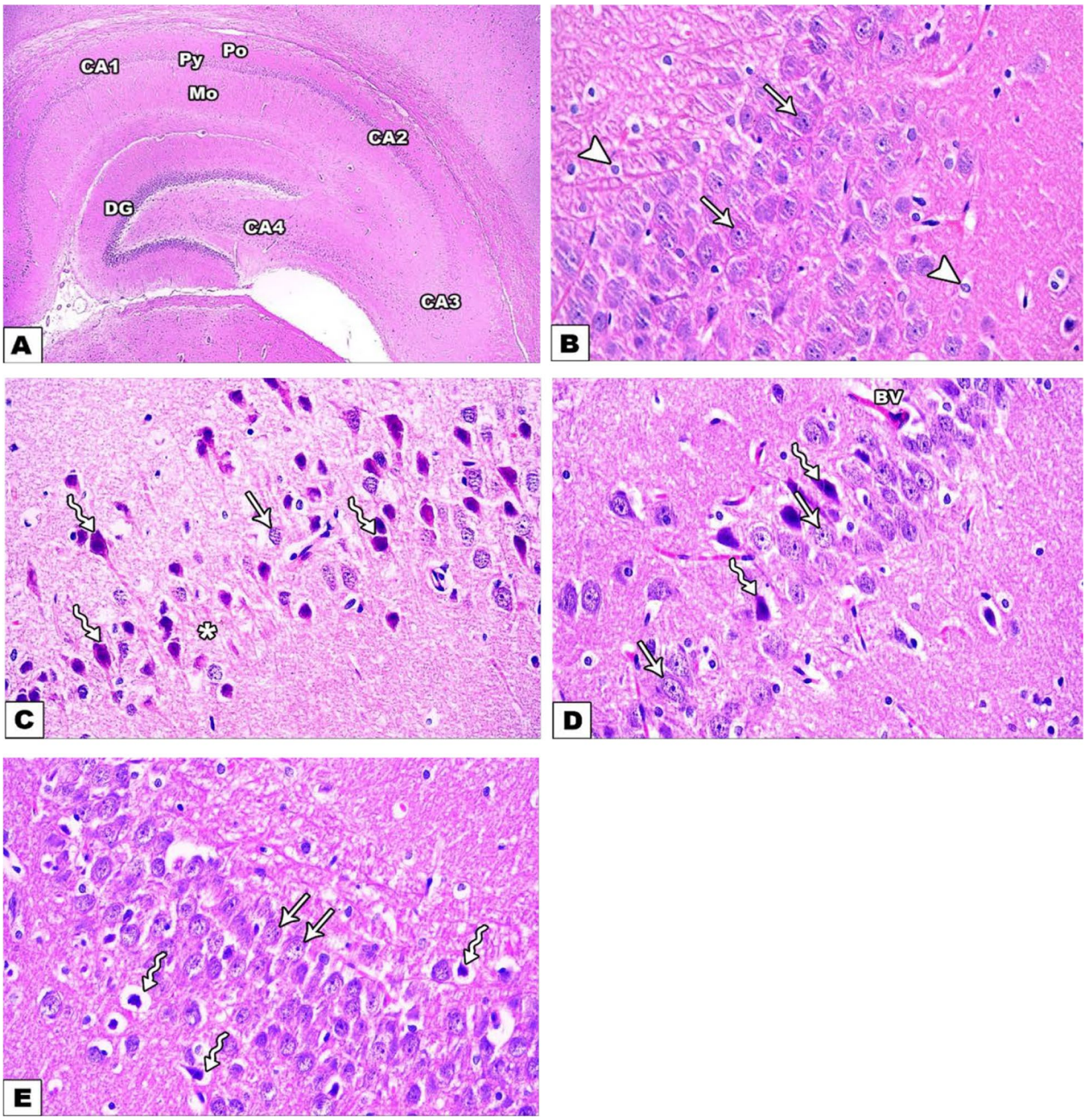

Fig. 6 photomicrographs of H&E stained sections of rat hippocampi of prenatally VPA-exposed male offspring.: **A**, B of the control group. **A** The Hippocampus comprises cornu ammonis regions: CA1, CA2, CA3, CA4. Each region is arranged into 3 layers: polymorphic (Po), pyramidal (Py), and molecular (Mo). The dentate gyrus (DG) appears enclosing CA4 (H& E × 40). **B** The pyramidal layer of the CA3 region contains large pyramidal cells with vesicular nuclei (arrows). Glial cells are also evident in molecular and polymorphic layers (arrowheads). **C** VPA-induced autism group: most of the pyramidal cells appear shrunken with darkly stained cytoplasm and pyknotic nuclei (zigzag arrows). Wide intercellular spaces can be observed (*). Few cells appeared normal (arrow). **D** Risperidone-treated group: most pyramidal cells appear normal with vesicular nuclei (arrows) except for some shrunken cells with darkly stained cytoplasm and pyknotic nuclei (zigzag arrows). Blood vessels can be seen (Bv). **E** Atorvastatin-treated group: numerous pyramidal cells are normal with vesicular nuclei (arrows), and only little shrunken cells appeared with darkly stained cytoplasm and pyknotic nuclei (zigzag arrows). (H& E × 400)

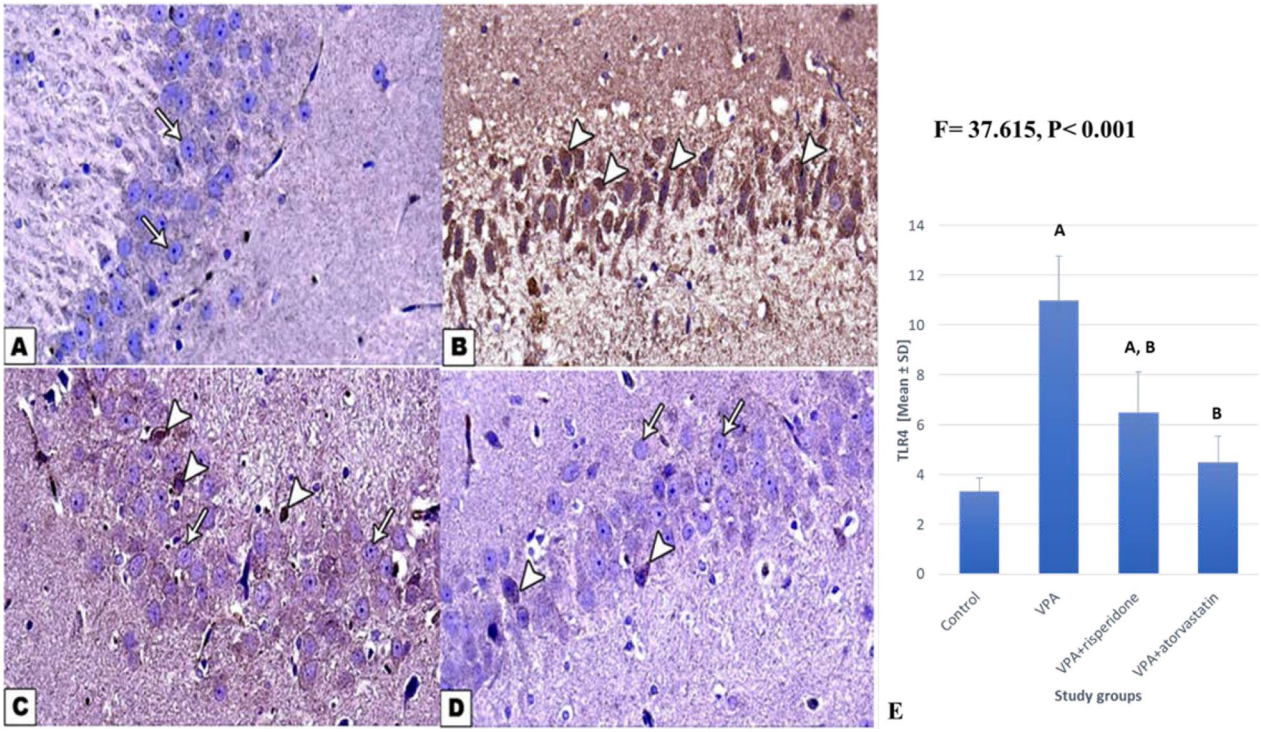

Fig. 7 Photomicrographs of TLR4-immunostained hippocampus sections in all study groups of prenatally VPA-exposed male offspring. **A** control group: pyramidal cells of CA3 region show negative immune reactions (arrows). **B** VPA induced autism group: pyramidal cells show strong positive immune reactions (arrowheads). **C** VPA-risperidone treated group, and **D** VPA-atorvastatin treated group: most pyramidal cells show negative immune reaction (arrows) except for a few cells with positive immune reaction (arrowheads) (immunostaining for TLR4 × 400). **E** Number of TLR4 positive cells of the CA3 region of the hippocampus in the study groups. Data are expressed as mean ± SD. One-way ANOVA and the post hoc Tukey's tests were used to compare the groups. **A** and **B** represent significance for the control and VPA groups, respectively. P value ≤ 0.05 is significant (P values significance of number of TLR4 positive cells with control, VPA, VPA + risperidone group respectively are: 0.001, 0.001, 0.079). VPA: valproic acid. TLR4; Toll-like receptor 4

one of the best broadly used tests to assess anxiety behavior in rodents. The most consistent measure of anxiety is the time spent in the light chamber [41]. In the current study, prenatal VPA exposure revealed a notable escalation in anxiety (decreased duration in the light chamber) compared with the control. In addition, the number of transitions between compartments was significantly higher in the VPA group, which may be related to anxiety or increased locomotion. Consistent with our findings, former studies have similarly shown anxiogenic effects in prenatal VPA-exposed rats [36, 42, 43], and they agree with clinical surveillance in which children and adults with ASD reveal apparent anxiety and socio-communicative impairment [44, 45]. Both risperidone and atorvastatin had an anxiolytic effect, which was significantly higher in the atorvastatin-treated group.

Finally, the open field test was conducted to evaluate anxiety and locomotor activity in patients with VPA-induced ASD. This test was used in several studies with variable outcomes. Some studies have stated that prenatally VPA-exposed rats exhibited reduced whole motor activity, while others demonstrated amplified motor activity [46]. In the current study, the VPA-exposed group exhibeted the hyperactive phenotype as evidenced by the increased total distance moved and the number of times they went to the centers. On the other hand, anxiety was shown in the VPA-exposed group by a significant increase in the stretched attended posture. Both risperidone and atorvastatin decreased hyperactivity and anxiety compared with VPA-induced autism. The crucial point is that atorvastatin reversed the hyperactive phenotype induced by VPA, and this inhibitory effect on hyperactivity isn't related to the inhibitory nature of atorvastatin, as it has shown increased locomotor activity in propionic acid-induced autism in rats in a previous study [39]. Mechanisms by which atorvastatin improves ASD behavioral disturbance remain unclear, but as reported in our research, this may be through the downregulation of TLR-4 expression with subsequent modulation of the disease.

TLRs are related to both innate and adaptive immunity and are crucial mediators of inflammatory responses

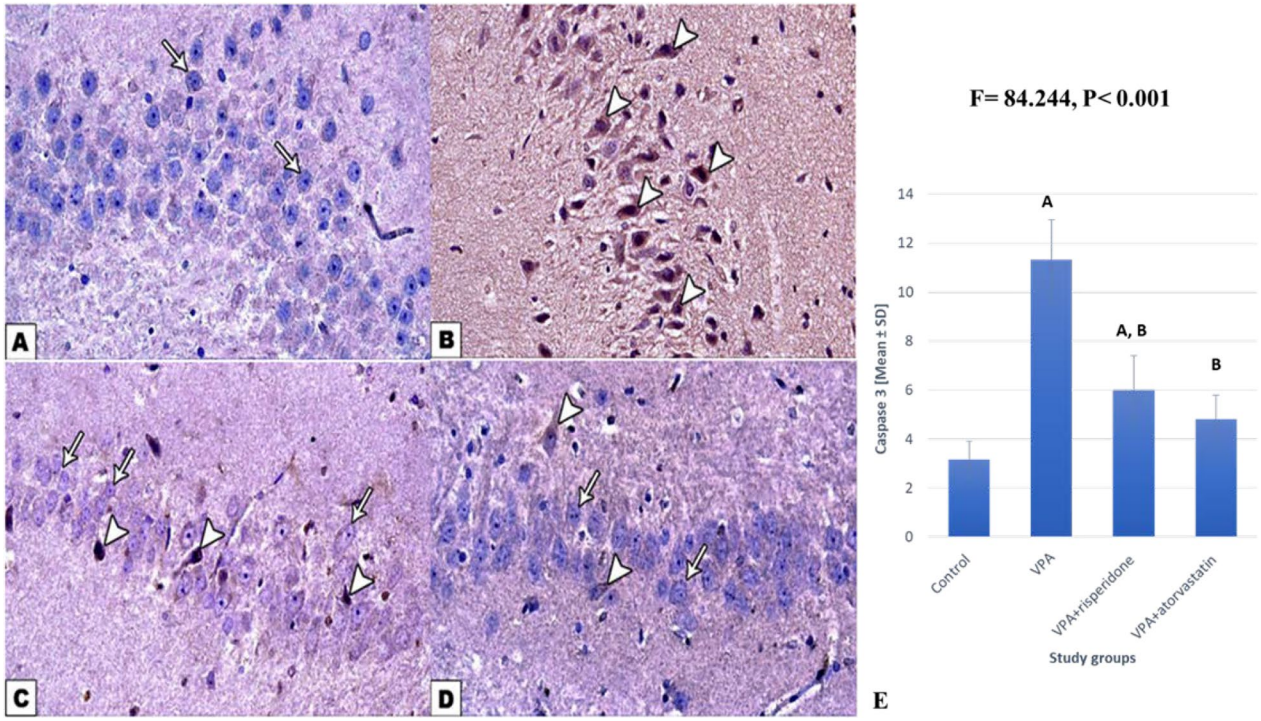

Fig. 8 Photomicrographs of Caspase-3 immunohistochemically stained hippocampus sections in all study group in prenatally VPA-exposed male offsprings. **A** Control group: pyramidal cells of the CA3 region show negative immune reaction (arrows). **B** VPA-treated group: pyramidal cells show strong positive immune reactions (arrowheads). **C** VPA-risperidone treated group, and **D** VPA-atorvastatin treated group: most of the pyramidal cells show negative immune reactions (arrows) except for a few cells with positive immune reactions (arrowheads). (Immunostaining for Caspase- 3 × 400). **E** Caspase- 3 positive cells number of CA3 region of the hippocampus in the study groups. Data are expressed as mean ± SD. One-way ANOVA and the post-hoc Tukey's tests were used to compare the groups; P value ≤ 0.05 is significant. (P values significance of number of caspase3 positive cells with control, VPA, VPA + risperidone group respectively are: 0.001, 0.001, 0.389). VPA: valproic acid

[47]. Impaired TLR function leads to an immune imbalance and further neuroinflammation [48]. In the CNS, TLR4 expression is augmented in the T cells of patients with ASD, and it mediates inflammatory activation in several neurodegenerative diseases [2, 48]. TLR-4 signaling activates the NFκB pathway which leads to the transcription of pro-inflammatory cytokines and ROS generation [8]**.** NFκB expression has also been shown to be increased both in peripheral blood and central nervous system in ASD patients [49]. Expression of TLR-4 with NFκB in autistic children may be a key mechanism for neuroinflammation in patients with ASD [2]. TLR4 stimulation activates microglia and leads to microglia-mediated inflammatory responses and cytokine creation and secretion by stimulating NF-κB through later gene transcription and protein synthesis [50, 51]. Microglial activation with the release of inflammatory mediators and ROS, further exacerbate microglial activation and recruit activated leukocytes and platelets, releasing granule content with more inflammatory markers. Endothelial injury and platelet adhesion contribute to blood-brain barrier (BBB) distraction with leak of endothelial content and increased infiltration of peripheral material, more aggravating neuroinflammation and glial activation [52].

Our study determines the role of TLR-4 signaling in the regulation of NFκB/NOX-2 derived ROS generation via the NFκB pathway in a rat model of VPA-induced autism through evaluation of TLR-4 gene expression by RT-PCR and its protein level via western blot, NFκB and NOX2 expression via RT-PCR and their protein level via ELISA, and finally detection of total ROS via ELISA.

Our study demonstrated that the VPA-induced autism group up-regulated TLR-4/NF-κB expression compared with the control group. Lamparter et al. demonstrated that VPA exposure amplified NF-κB transcriptional activity and can facilitate VPA-induced teratogenesis [53]. NF-κB is a transcription factor that alters the expression of several genes involved in immune and inflammatory responses [54].

Risperidone and atorvastatin administration to offspring exhibited a significant decline in TLR-4 and NF-κB compared with the VPA-induced autism group. Yousefi-Manesh et al. confirmed the ameliorating effect of risperidone on acetic acid-induced colitis in rats through

suppression of the TLR4 and NF-κB signaling pathways [55]. Risperidone can adjust the cell-mediated immune responses, chemokine, and lymphocytes to correct its effects on autoimmune and inflammatory status [56]. Statins also efficiently depress TLR4 activity and consequently downregulate inflammatory pathways to decline inflammation in vascular and nonvascular systems [57]. Amassing evidence suggests that the beneficial effects of statins may depend on targeting TLR4. The impact of statins on the central receptors in the inherent immunity system and regulation of the TLR4 signaling pathway can be attributed to their beneficial effects in numerous disorders, including colitis, renal tubular injury, CV, arthritis, and brain injury [58]. Yang et al. showed that atorvastatin inhibits TLR4 gene transcription TLR4 and inhibits its protein level, resulting in decreased tumor necrosis factor-alpha (TNF-α), interleukin 6 (IL-6), and IL-1β levels [25].

As previously described by Nadeem et al., increased TLR-4 expression and NF-κβ activation in autistic children are linked with enhanced NOX2/ROS signaling [2]. In our study, animals in the VPA-treated group showed a significant increase in NOX2/ROS levels compared with the control group. Azirak et al., reported elevated NOX2 levels following VPA treatment [59]. NOX2 enzymes are concerned with oxidative stress increase, which is recognized in various brain illnesses, from psychiatric to neurodegenerative diseases [60].

NOX facilitates electron transmission across plasma membranes to O2 and produces superoxide and other ROS downstream [61]. In addition, extreme NOX activity leads to apoptotic cell death and participates in neurodegeneration [62]. Risperidone and atorvastatin administration significantly decreased NOX2/ROS levels compared with the untreated group, and atorvastatin significantly reduced NOX2 levels compared with the risperidone group. This result in concomitates with other previous studies [63, 64]. Statins lower NOX2 and superoxide production and reduce inflammatory cell infiltration [65].

ROS signals stimulate the assembly of inflammatory genes and induce apoptosis through CAS-3 upregulation [11, 66]. CAS-3 is a protease with a well-known role in apoptosis [67]. Neurodegenerative diseases have high CAS-3 levels, which are determined in postmortem brain tissue [68, 69]. It has been established that CAS-3 expression is high in the cerebellum of individuals with autism[70]. Moreover, previous studies in mice have proposed that VPA exposure causes higher expression of apoptotic markers and is assumed to be a grave cause of neural tube defects and altered embryonic signaling pathways [71]. Thus, in the existing study, immunostaining for CAS-3 in the hippocampus of the VPA group showed a strong positive reaction, which is consistent with the study by Azirak et al. [58]. Both risperidone and atorvastatin treatment resulted in a remarkable reduction of CAS-3, suggesting their anti-apoptotic effects. Abekawa et al. reported that risperidone has an anti-apoptotic effects [72]. Moreover, atorvastatin has an antiapoptotic and mitigating effects on CAS-3 [24, 73].

Finally, histological analysis of the hippocampus revealed CA regions that were alleviated in the treated groups. The atorvastatin-treated group showed more improvement than the risperidone group, in which numerous pyramidal cells were normal with vesicular nuclei and only little shrunken cells; neuronal survival is noticeably better in the atorvastatin group. Piermartiri et al. [74] reported the neuroprotective effect of atorvastatin and its ability to prevent hippocampal cell death and structural alteration following amyloid-β1–40 administration in mice. Moreover, Durankuş et al. [39] demonstrated the protective effects of atorvastatin on neurons subjected to PPA-induced damage in the rat cerebellum. Atorvastatin is a relatively small compound that can cross BBB. Once it penetrates the brain parenchyma, it not only affects cholesterol biosynthesis but also affects neuronal and glial cells, neurotransmitter levels, synapse receptors, cellular viability, neuronal dendrites and oligodendrocyte-mediated myelination [75]. Thus, it is evident that atorvastatin has a remarkable neuroprotective effect against neurological diseases through its pleiotropic effects and could be a potential therapeutic agent against such diseases, including autism, which requires further research. Our results suggest that atorvastatin targeting of TLR-4/NF-κB/NOX2 and the apoptosis signaling pathway could alleviate and modify ASD, which requires further confirmation.

Conclusion

This study revealed that prenatally VPA-exposed male offspring showed several autism features including behavioral, biochemical, and hippocampal histological alterations, which could be related to the activation of the TLR4/ NF-κB/NOX2 molecular pathway with subsequent neuronal apoptosis. Both risperidone and atorvastatin treatment significantly decreased VPA-induced behavioral impairment, neuroinflammation, oxidative dysfunction, and apoptosis, presumably by downregulating TLR-4/NF-κB/NOX2 and apoptotic pathway. The improvement was more significant in the atorvastatin-treated group than in the risperidone-treated group. Atorvastatin could be a prospective drug that alleviates ASD through its effects on the TLR4/ NF-κB/NOX2 pathway.

Limitations of the study

The findings of this study have a few limitations. First, we determined the VPA induced autism model only in male rats; since ASD is more prevalent in males, the extrapolation of our results in females had to be explored and compared with the results in males. Furthermore, to confirm the hypothesis that TLR4/ NF-κB signaling pathway participates in prenatally VPA-induced autism, TLR 4 and NF-κB antibodies evaluation in brain different sites as in the striatum and prefrontal cortex, would be a great tool. Furthermore, the autism cell lines and culture can be used to evaluate the TLR4/ NF-κB signaling pathway and effect of atorvastatin and risperidone.

Materials and methods

Drugs

Drugs were obtained from Sigma-Aldrich Co. (St. Louis, MO, USA) in the following powder form: sodium valproate (VPA. CAS Number 1069-66-5); risperidone (CAS Number 106266-06-2); and atorvastatin (CAS 134523-03-8). Atorvastatin was chosen among statins because it is lipophilic and can cross the blood-brain barrier [76].

Animals

Twenty adult Sprague-Dawley pairs (200–250g) were acquired from the Medical Experimental Research Center (MERC), Faculty of Medicine, Mansoura University. Fifty offspring rats were obtained from male and female mating rats. Male offspring (about twenty-four) were taken for this study. Rats were housed in plastic cages with sawdust bedding (40 × 26 × 20 cm; l × w × h). Rats were fed a clean, wholesome, fresh, and nutritious pelleted diet and were watered from water bottles with sipper tubes. Rats were maintained on a 12h:12h circadian cycle with lights on at 06:00 and a constant temperature (22 ± 2°C) and humidity (55 ± 5%). Animal treatment and maintenance were carried out following the "Guide for the Care and Use of Laboratory Animals" conveyed via the Institution of Laboratory Animal Research and available by the National Research Council, USA, 2010. The research protocol was approved by the Institutional Review Board (IRB) of Mansoura Faculty of Medicine. Ethical code: R.21.11.1506. All exertions were performed to reduce animal numbers and distress.

Experimental design

Prenatal induction of autism: According to Kumar and Sharma, mature female rats were coupled overnight, and the following morning, a vaginal smear using light microscopy was performed [77]. Rats with vaginal lumps or sperm within the vaginal swap were confirmed on-gestational day (GD) 1 when the vaginal plug was detected. Two pregnant females received saline in GD 12.5; the male offsprings (n = 6) born from these were used in the control normal group, and eight pregnant females in GD 12.5 were administered a solitary intraperitoneal (IP) injection of VPA (500 mg/kg, melted in 2 ml of normal saline); the male offsprings (n = 18)born from these were used for experimental groups; VPA induced autism, VPA+ risperidone, and VPA+ atorvastatin groups). Pregnant Females were housed individually until delivery, and the assumed day was zero postnatal day (PND 0). The average number of pups from single mothers varied from 7 to 9 with male pups from 5 to 6. They were permitted to raise their offspring until weaning, PND 21. Only male offspring were used in this study to eliminate the effects of altered gender on outcomes. This selection aligns with previous research reporting that prenatally VPA-treated male descendants reliably displayed marked diminution in social interaction compared with female offspring [36, 78, 79].

Twenty-four male offspring (48-50 gm) were divided at PND 21 into four equal groups as follows (Fig. 9): *1-Control group (n = 6)* male offsprings born to females received saline in GD 12.5 treated with vehicle (0.5% v/v methylcellulose from PND21to PND51); *2-VPA-induced autism group* (n = 6) male offsprings born to female received VPA in GD 12.5 (500 mg/kg melted in 2 ml of normal saline) [31, 77, 79], treated with vehicle (0.5% v/v methylcellulose from PND21to PND51); *3-VPA+ risperidone group* (n = 6), male offsprings born to female received VPA in GD 12.5 (500 mg/kg melted in 2 ml of normal saline) [31, 77, 79], treated with oral risperidone (1 mg/kg/day suspended in 0.5% v/v methylcellulose from PND21to PND51) [80–82] and *4-VPA+ atorvastatin group* (n=6) male offspring born to the female received VPA in GD 12.5 (500 mg/kg melted in 2 ml of normal saline) [31, 77, 79], and were treated with oral atorvastatin (20 mg/kg daily suspended in 0.5% v/v methylcellulose from PND21to PND51) [83, 84]. Vehicle and drug suspensions were administered via gavage 5 ml/kg once daily.

All rats received vehicles or drugs from PND21 to PND51, and no deaths were recorded. It has been established that initial interferences directing ASD social deficits are essential to improve the long-standing consequences of the disease. The period from PND21 to PND51 targets a perilous period of neurodevelopment when regulating neuronal activity; strength repairs neurodevelopmental plasticity to manage autism-like behaviors [31].

Behavioral tests

The rats were trained for two sequential days. Two days before sacrifice, the tests were completed. The tools

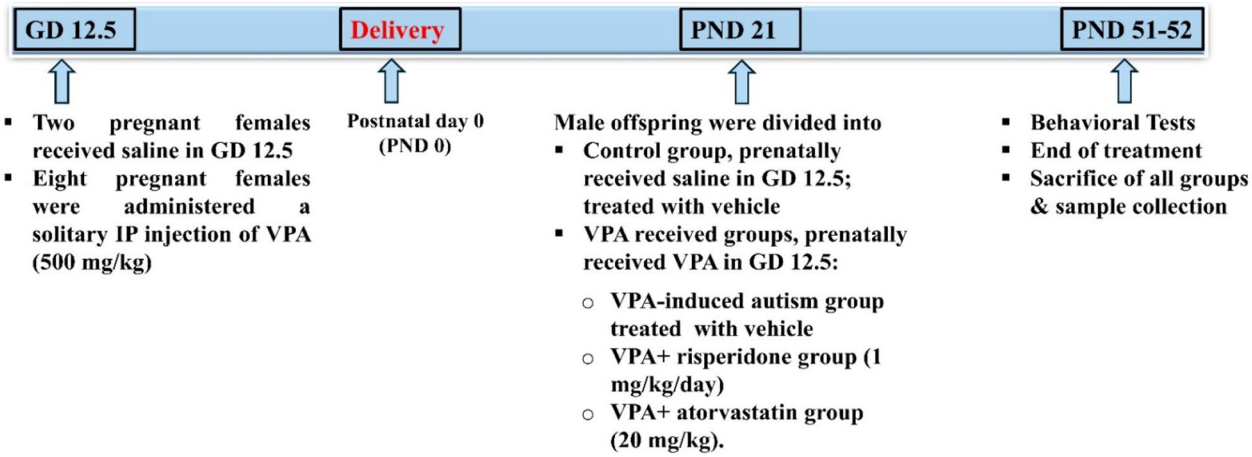

Fig. 9 Study design and experimental grouping

were thoroughly cleaned with 70% ethanol and water for each test and were left to dry. All trials were conducted between 10:00 am and 2:00 pm. The tests and behaviors of the rats were documented using a video camera and analyzed using two blinders.

Three chamber test

The three-chamber test was used to assess rodent sociability. The apparatus is a rectangular, 3-chambered box prepared from translucent Plexiglas with a detachable floor and barriers. Every chamber measured 30 cm L× 60 cm W×35 cm H. This test evaluates the preference for interacting with a social (S) stimulus versus a non-social (NS) stimulus. The trial was conducted in three phases. In the 1st phase (habituation), the test rat was habituated in the middle of a three-chamber apparatus containing two empty cups to reduce the salience of these objects. Next, two identical objects (paper balls) were placed within the cups to familiarize the animal with the objects contained within the cups (pre-test phase). Finally, a social stimulus (an age- and sex-matched rat) is introduced under one cup, and a novel non-social stimulus (wooden block) is placed under the other cup (test phase) [1]. Then, the 2 entries were opened to permit the test rat in the middle to freely discover each of the 3 chambers for 10 mins. Processes were recorded to determine the latency, the duration consumed in each chamber, the number of entries into each chamber, and the time consumed in direct contact with the novel rat [85].

Dark-light box test

Anxiety behavior was estimated using dark-light box tests as described by Castelhano-Carlos et al. [86]. The test was based on the native affinity of rats to the illuminated area and their impulsive exploratory behavior. Anxiety is understood when rats tend to remain in dim regions for a prolonged duration. The dark-bright box was executed in a box with 2 parts (MazeEngineers, USA). The test box (51 length × 51 width × 40 cm height) contained one more significant bright part (51 × 34.5 × 40 cm) lit up by a white fluorescent lamp (400 lux at the box floor) and a smaller dark compartment (51 × 16.5 × 40 cm). The 2 parts were linked by a slit opening (7.5 cm × 8.5 cm). The rats were positioned in the middle of the illuminated area at the start of the test, and the test was conducted for 5 minutes. Two parameters were assessed: the time spent in the bright vs. the dark compartment, calculated in seconds, and the number of transitions between the 2 chambers.

Open field test

Motor performance and anxiety levels in rats were estimated using an open-field test [87, 88]. The apparatus was prepared of white plywood with 72 × 72-cm floor measurements and 36-cm high walls. One of the walls and floor were made of transparent Plexiglas; thus, rats could be followed inside the apparatus. The blue lines separate the floor into 16 squares (18 × 18 cm). On the test day, the rats were transported to the test room and allowed to adjust to the room before testing [82]. Rats were gently positioned by qualified detectives in one of the four corners of the apparatus, and they were permitted to search the perimeter freely within a certain period (5 minutes) [89]. The rats were then reverted to their home cages. The distance traveled (number of square participants), the number of times rats went

to the center, and stretch attendance positions were assessed [90, 91].

Brain tissue preparation

A day after behavioral testing, the rats were rapidly decapitated. The brains were quickly separated, placed on ice, and severed into two hemispheres without discernment. The hippocampus was separated from the right hemisphere and divided into two parts. One part was immediately fully submerged in RNA*later*™ *(Qiagen, Germany)*, using 10 μL reagent per 1 mg of tissue [92]. The submerged tissue samples were incubated overnight at 4 °C, followed by storage at − 80 °C until gene and protein expression detection. The other part of the right hippocampus was carefully soaked in ice and weighed in on analytical balance. A 10% homogenate was prepared in 0.05 M phosphate buffer (pH 7) using a polytron homogenizer at 4 °C. The homogenate was centrifuged at 10,000 rpm for 20 minutes to eliminate cell debris, RBCs, unbroken cells, mitochondria, and nuclei. The supernatant (cytoplasmic extract) was aliquoted and stored at -20^{0}C for subsequent assessment of ROS, NOX2 &NFκB. The left hemisphere was fixed by soaking in 10% neutral buffered formalin, dehydrated in rising grades of alcohol, cleared in xylene, and finally inserted in paraffin for routine histological examinations. Neuropathology of the amygdala and hippocampus was first observed in a postmortem study of autism. Up to now, abnormalities of the amygdala and hippocampus have been implicated in autism-associated deficits [93]. Banker et al. reported that structural variations in the hippocampal structure likely have a more significant impact on social dysfunction [94].

Biochemical and molecular evaluation

Real-time quantitative polymerase reverse transcription polymerase chain reaction (RT-PCR)

After homogenization by liquid nitrogen, total cellular RNA was extracted from all tissue samples using QIAzol® lysis reagent (Qiagen, Germany) according to the protocol of Chomczynski [95]. The RNA concentration and purity of each sample were determined using a NanoDrop 2000c Spectrophotometer (Thermo Scientific, USA). The extracted RNA samples were then kept at -80∘C until reverse transcription. The synthesis of complementary DNA (cDNA) from 1 μg of total RNA was done using the SensiFAST™ cDNA Synthesis Kit *(Bioline, UK)* according to the manufacturer's instructions. The reaction was carried out using the Applied Biosystems® 2720 thermal cycler *(Applied Biosystems, USA)* as follows: primer annealing at 25 °C for 10 min, reverse transcription at 45 °C for 15 min, and inactivation at 85°C for 5 minutes. The cDNA samples were stored at − 20 °C. The cDNA was subjected to a real-time PCR assay established using the technique described by Freeman et al. [96]. RT-qPCR was performed by the Applied Biosystem® 7500 Real-Time PCR Systems *(Applied Biosystems, USA)*, using the *HERA^{PLUS}* SYBR® Green qPCR master mix *(Willowfort, UK)*. All primers were synthesized by Vivantis Technologies, Selangor Darul Ehsan, Malaysia. The primer sequences used were: TLR4 Forward, 5′- CCGTCACCACATACTGCCTTTA-3′ and reverse, 5′- GCAGTTTGGACTATTGAAATACGA AA-3′; NOX2 Forward, 5′- TTGTGGCACACTTGT TCAACCTGG-3′ and reverse, 5′- TCACACGCATAC AAGACCACAGGA -3′, NF-κB Forward, 5′- GTCTCA AACCAAACAGCCTCAC -3′ and reverse, 5′- CAG TGTCTTCCTCGACATGGAT -3′and *GAPDH* Forward, 5′- CACCCTGTTGCTGTAGCCATATTC -3′ and reverse, 5′- GACATCAAGAAGGTGGTGAAGCAG-3′. The mix was made as follows: 6 μL RNase-free water, 1 μL sense primer (10 pmol/μL), 1 μL antisense primer (10 pmol/μL), 10 μL *HERA^{PLUS}* SYBR® Green qPCR master mix (2X), and 2 μL of cDNA (50 ng/μL), in a total volume of 20 μL. The following program was used: initial denaturation at 95 °C for 3 minutes, followed by 40 cycles of denaturation at 95 °C for 10 seconds, and annealing/extension at 60 °C for 30 seconds. TLR4, NOX2, and NF-κB mRNA expression levels were normalized to that of the housekeeping gene GAPDH, and relative expression levels were detected using the ($2^{-\Delta\Delta ct}$) method [97].

Western blot analysis

Total protein was extracted using the QIAzol reagent following the manufacturer's specifications and then quantified using a Bradford protein assay kit (Bio-Rad, USA). 20 µg proteins of each sample were then loaded with an equal volume of 2x Laemmli sample buffer. The pH was checked and brought to 6.8. Each previous mixture was boiled at 95 °C for 5 min to ensure protein denaturation before loading on polyacrylamide gel electrophoresis. Polyacrylamide gels were performed using TGX Stain-Free™ FastCast™ Acrylamide Kit (SDS-PAGE) (cat# 161–0181; Bio-Rad Lab, USA). The SDS-PAGE TGX Stain-Free FastCast was prepared according to manufacturer instructions. The gel was assembled in a transfer sandwich as follows from below to above (filter paper, polyvinyl difluoride, gel, and filter paper). The sandwich was placed in the transfer tank with 1x transfer buffer, composed of 25 mM Tris, 190 mM glycine, and 20% methanol. Then, the blot was run for 7 min at 25 V to allow the protein bands to transfer from the gel to the membrane using BioRad Trans-Blot Turbo. Nonspecific binding was blocked with tris-buffered saline with Tween 20 buffer and 3% bovine serum albumin at room temperature for 1 h. The blot was rinsed 3–5 times

for 5 min with TBST. The membranes were incubated with TLR4 (H-80) rabbit polyclonal antibody (1:1000, #sc-10741, Santa Cruz, USA) overnight at 4 °C. The blot was rinsed 3–5 times for 5 min with TBST. Finally, the membranes were incubated with HRP-conjugated goat anti-rabbit IgG secondary antibody (1:5000, #NB7156, Novus Biologicals, USA) for 1 h at room temperature. Protein bands were identified using a Clarity TM Western ECL substrate (Bio-Rad cat#170-5060) and visualized by chemiluminescence using a ChemiDoc MP Imager (Bio-Rad, USA). Image analysis software was used to read the band strength of the target proteins against β-actin (housekeeping protein).

Enzyme-Linked Immune Sorbent Assay

The levels of ROS, NOX2, and NF-κB were determined in cytoplasmic extract using ROS ELISA kit (cat.no. E1924r; EIAab, Wuhan, China), CYBB/NOX2/gp91phox sandwich ELISA kit (cat. no. LS-F39030; LSBio, WA, USA), and NF-κB assay kit (cat. no. SEA616Ra; Cloud-Clone Corp., Wuhan, China), following the manufacturer's protocol.

Histological examination

- Hematoxylin and eosin staining: Sections of 5 μm thickness were obtained by rotatory microtome and were fixed on glass slides. Slices were deparaffinized in xylene, dehydrated in alcohol in descendent grades, and then stained with H&E [98].
- Immunohistochemical examination: The slices were deparaffinized and rehydrated, then hydrogen peroxide (0.3%) was administered to suppress endogenous peroxidase activity. Unmasking of the antigenic peptide was performed by placing the slides in a plastic bottle filled with citrate buffer PH 6.0, and boiling the slides in a microwave oven at 100 °C for 10 min. The slides were raised overnight at 4 °C with the following primary antibodies: anti-caspase-3 antibody for the detection of caspase-3 protein level in neurons; a marker of apoptosis (dilution 1:500, rabbit polyclonal IgG, service bio, USA), antiTLR4 antibody for the detection of TLR4 protein levels in neurons; immune marker that mediates inflammation (dilution 1:500, mouse monoclonal IgG, service bio, USA). Biotinylated secondary antibodies were used, followed by the avidin–biotin complex. Finally, diaminobenzidine (DAB) was used as a chromogen (Dakopatts, Glostrup, Denmark), and the slides were counterstained with hematoxylin solution. Apoptotic cells were detected by caspase-3 immunostaining, whereas TLR4 expression was assessed by TLR4 immunostaining. Negative controls were prepared by applying the same steps except for the use of primary antibody [99].
- Morphometric study: An image analyzer computer system was used to assess the following parameters: a) CAS-3-positive and b) TLR4-positive cell numbers. For each group, the cells were counted in five randomly chosen nonoverlapping, high-power fields (magnification × 400) in each section from six rats in each group. The images were evaluated on an Intel® Core I3® computer using Video Test Morphology® software (Russia) (Mansoura University).

Statistical analysis

SPSS software (version 25.0, IBM, Chicago, IL, USA) was used to analyze the data. Assumptions of normality in each group and homogeneity of variances were verified using the Shapiro-Wilk test and Levine's test, respectively. Data were expressed as mean ± SD. The one-way ANOVA test was used to compare the means of the 4 study groups, and the post-hoc Tukey's test was used for numerous comparisons of the group means. P values less than 0.05 was considered significant.

Abbreviations

ASD	Autism spectrum disorder
BBB	Blood–brain barrier
CA	Cornu Ammonis
CAS-3	Caspase 3
ELISA	Enzyme-Linked Immunosorbent Assay
FDA	Food and Drug Administration
GD	Gestational day
H&E	Hematoxylin and eosin
HMG-CoA	Hydroxy-3-methylglutaryl co-enzyme A
IL	Interleukin
IP	Intraperitoneal
MERC	Medical Experimental Research Center
NF-κB	Nuclear factor kappa-light-chain enhancer of activated B cells
NOX2	Nicotinamide adenine dinucleotide phosphate (NADPH) oxidase 2
PND	Postnatal day
ROS	Reactive oxygen species
RT-PCR	Reverse transcription polymerase chain reaction
TLR	Toll-like receptor
TNF-α	Tumor necrosis factor-alpha
VPA	Valproic acid
WB	Western blot

Acknowledgements

The authors show their gratitude to the Deanship of Scientific Research at King Khalid University for funding this work through a large group Research Project under grant number RGP2/262/45.

Author contributions

E.F[1] contributed to the study conception, design and data collection. E.F.[1], M.A[2], Z.A[2] behavioral testes and analysis. A.M[13] biochemical analysis. S.M.[3] and M.E.[9,10] histopathological and immunohistochemical assay and analysis. E.A.[4] and E.A.[5] collected, wrote results, and prepared figures E.E[6]., F.A.[7], A.N.[8], and A.E. [11,12] contributed to statistical analysis, project administration and funding acquisition. All authors wrote, revised and approved the final manuscript.

Funding
This work was funded by the Deanship of Scientific Research at King Khalid University for funding this work through the large group Research Project under grant number RGP2/262/45.

Availability of data and materials
No datasets were generated or analysed during the current study.

Declarations

Ethics approval and consent to participate
The Mansoura Faculty of Medicine's Institutional Review Board (IRB) reviewed and approved the animal study, which was conducted according to the guidelines of the National Research Council's Guide for the Care and Use of Laboratory Animals.

Competing interests
The authors declare no competing interests.

Author details
[1]Department of Clinical Pharmacology, Faculty of Medicine, Mansoura University, Mansoura 31516, Egypt. [2]Department of Medical Physiology, Faculty of Medicine, Mansoura University, Mansoura, Egypt. [3]Department of Medical Histology and Cell Biology, Faculty of Medicine, Mansoura University, Mansoura, Egypt. [4]Department of Pediatrics, Faculty of Medicine, Mansoura, University, Mansoura, Egypt. [5]Department of Forensic Medicine and Clinical Toxicology, Faculty of Medicine, Mansoura University, Mansoura, Egypt. [6]Department of Anatomy, College of Medicine, King Khalid University, 62529 Abha, Saudi Arabia. [7]King Fahad Armed Forces Hospital, Khamis Mushatt, Saudi Arabia. [8]Bin Rushed Center, Khamis Mushait, Saudi Arabia. [9]Department of Basic Medical Sciences, College of Medicine, AlMaarefa University, 13713 Diriyah, Riyadh, Saudi Arabia. [10]Department of Human Anatomy and Embryology, Faculty of Medicine, Mansoura University, Mansoura 35516, Egypt. [11]Department of Zoology, Faculty of Science, Damanhour University, Damanhour, Egypt. [12]Al Rayan National College of Medicine, Hejrah Street-Madinah, P.O. Box 41411, Al-Madinah, Kingdom of Saudi Arabia. [13]Department of Medical Biochemistry, Faculty of Medicine, Mansoura University, Mansoura, Egypt.

Received: 26 April 2024 Accepted: 1 September 2024
Published: 30 September 2024

References

1. Rein B, Ma K, Yan Z. A standardized social preference protocol for measuring social deficits in mouse models of autism. Nat Protoc. 2020;15(10):3464–77.
2. Nadeem A, et al. Toll-like receptor 4 signaling is associated with upregulated NADPH oxidase expression in peripheral T cells of children with autism. Brain Behav Immunity. 2017;61:146–54.
3. Ebrahimi Meimand S, Rostam-Abadi Y, Rezaei N. Autism spectrum disorders and natural killer cells: a review on pathogenesis and treatment. Expert Rev Clin Immunol. 2021;17(1):27–35.
4. Sabra A, Aderbal Filho S, Selma S. Autism: etiology, epidemiology, pathology, clinical aspects and treatment. Autism Open Access. 2020;10(3):253.
5. Bergeron JD, et al. White matter injury and autistic-like behavior predominantly affecting male rat offspring exposed to group B streptococcal maternal inflammation. Dev Neurosci. 2013;35(6):504–15.
6. Hsiao EY, et al. Modeling an autism risk factor in mice leads to permanent immune dysregulation. Proc Natl Acad Sci USA. 2012;109(31):12776–81.
7. Lucas K, Maes M. Role of the toll like receptor (TLR) radical cycle in chronic inflammation: possible treatments targeting the TLR4 pathway. Mol Neurobiol. 2013;48(1):190–204.
8. Bueno BG, et al. Innate immune receptor Toll-like receptor 4 signalling in neuropsychiatric diseases. Neurosci Biobehav Rev. 2016;64:134–47.
9. Vallabhapurapu S, Karin M. Regulation and function of NF-κB transcription factors in the immune system. Annu Rev Immunol. 2009;27:693–733.
10. Hsieh HL, Yang CM. Role of redox signaling in neuroinflammation and neurodegenerative diseases. Biomed Res Int. 2013;2013(1): 484613.
11. Yang CM, et al. Multiple factors from bradykinin-challenged astrocytes contribute to the neuronal apoptosis: involvement of astroglial ROS, MMP-9, and HO-1/CO system. Mol Neurobiol. 2013;47(3):1020–33.
12. Tummers B, Green DR. Caspase-8: regulating life and death. Immunol Rev. 2017;277(1):76–89.
13. Heckmann BL, Tummers B, Green DR. Crashing the computer apoptosis vs. necroptosis in neuroinflammation. Cell Death Differ. 2019;26(1):41–52.
14. Emberti Gialloreti L, Curatolo P. Autism spectrum disorder: why do we know so little? Front Neurol. 2018;9:394207.
15. Mano-Sousa BJ, et al. Effects of risperidone in autistic children and young adults: a systematic review and meta-analysis. Curr Neuropharmacol. 2021;19(4):538–52.
16. Marchezan J, et al. Immunological dysfunction in autism spectrum disorder: a potential target for therapy. NeuroImmunoModulation. 2019;25(5–6):300–19.
17. Sharma SR, Gonda X, Tarazi FI. Autism spectrum disorder: classification, diagnosis and therapy. Pharmacol Ther. 2018;190:91–104.
18. Kandezi N, et al. Novel insight to neuroprotective potential of curcumin: a mechanistic review of possible involvement of mitochondrial biogenesis and PI3/Akt/ GSK3 or PI3/Akt/CREB/BDNF signaling pathways. Int J Mol Cell Med. 2020;9(1):1–32.
19. Pella D, Rybar R, Mechirova V. Pleiotropic effects of statins. Acta Cardiol Sin. 2005;21(4):190.
20. Katsargyris A, et al. Statin treatment is associated with reduced toll-like receptor 4 immunohistochemical expression on carotid atherosclerotic plaques: a novel effect of statins. Vascular. 2011;19(6):320–6.
21. Pan HC, et al. Neuroprotective effect of atorvastatin in an experimental model of nerve crush injury. Neurosurgery. 2010;67(2):376–88 (**discussion 388–9**).
22. Chen JH, et al. An early neuroprotective effect of atorvastatin against subarachnoid hemorrhage. Neural Regen Res. 2020;15(10):1947–54.
23. Kho AR, et al. The effects of atorvastatin on global cerebral ischemia-induced neuronal death. Int J Mol Sci. 2021;22(9):4385.
24. Yu L, et al. Atorvastatin inhibits neuronal apoptosis via activating cAMP/PKA/p-CREB/BDNF pathway in hypoxic-ischemic neonatal rats. FASEB J. 2022;36(4): e22263.
25. Yang SS, et al. Atorvastatin decreases Toll-like receptor 4 expression and downstream signaling in human monocytic leukemia cells. Cell Immunol. 2012;279(1):96–102.
26. Denucci BL, et al. Current knowledge, challenges, new perspectives of the study, and treatments of Autism Spectrum Disorder. Reprod Toxicol. 2021;106:82–93.
27. Xu X, et al. Anti-inflammatory and immunomodulatory mechanisms of atorvastatin in a murine model of traumatic brain injury. J Neuroinflammation. 2017;14(1):167.
28. Mabunga DF, et al. Exploring the validity of valproic acid animal model of autism. Exp Neurobiol. 2015;24(4):285–300.
29. Nicolini C, Fahnestock M. The valproic acid-induced rodent model of autism. Exp Neurol. 2018;299(Pt A):217–27.
30. Chaliha D, et al. A systematic review of the valproic-acid-induced rodent model of autism. Dev Neurosci. 2020;42(1):12–48.
31. Atia AA, et al. The comparative effectiveness of metformin and risperidone in a rat model of valproic acid-induced autism, potential role for enhanced autophagy. Psychopharmacology. 2023;240(6):1313–32.
32. Roullet FI, Lai JK, Foster JA. In utero exposure to valproic acid and autism—a current review of clinical and animal studies. Neurotoxicol Teratol. 2013;36:47–56.
33. Mirza R, Sharma B. Benefits of fenofibrate in prenatal valproic acid-induced autism spectrum disorder related phenotype in rats. Brain Res Bull. 2019;147:36–46.
34. Markram K, et al. Abnormal fear conditioning and amygdala processing in an animal model of autism. Neuropsychopharmacology. 2008;33(4):901–12.
35. van Steensel FJ, Bogels SM, Perrin S. Anxiety disorders in children and adolescents with autistic spectrum disorders: a meta-analysis. Clin Child Fam Psychol Rev. 2011;14(3):302–17.
36. Schiavi S, et al. Reward-related behavioral, neurochemical and electrophysiological changes in a rat model of autism based on prenatal exposure to valproic acid. Front Cell Neurosci. 2019;13:479.

37. Hara Y, et al. Risperidone and aripiprazole alleviate prenatal valproic acid-induced abnormalities in behaviors and dendritic spine density in mice. Psychopharmacology. 2017;234(21):3217–28.
38. Elnahas EM, et al. Novel role of peroxisome proliferator activated receptor-alpha in valproic acid rat model of autism: mechanistic study of risperidone and metformin monotherapy versus combination. Prog Neuropsychopharmacol Biol Psychiatry. 2022;116: 110522.
39. Durankuş F, et al. Atorvastatin improves the propionic acid-induced autism in rats: the roles of sphingosine-1-phosphate and anti-inflammatory action. Cureus. 2023;15(3): e36870.
40. Mingins JE, et al. Anxiety and intellectual functioning in autistic children: a systematic review and meta-analysis. Autism. 2021;25(1):18–32.
41. Tucker LB, McCabe JT. Measuring anxiety-like behaviors in rodent models of traumatic brain injury. Front Behav Neurosci. 2021;15: 682935.
42. Servadio M, et al. Impaired repair of DNA damage is associated with autistic-like traits in rats prenatally exposed to valproic acid. Eur Neuropsychopharmacol. 2018;28(1):85–96.
43. Sailer L, et al. Consequences of prenatal exposure to valproic acid in the socially monogamous prairie voles. Sci Rep. 2019;9(1):2453.
44. Dworzynski K, et al. How different are girls and boys above and below the diagnostic threshold for autism spectrum disorders? J Am Acad Child Adolesc Psychiatry. 2012;51(8):788–97.
45. Head AM, McGillivray JA, Stokes MA. Gender differences in emotionality and sociability in children with autism spectrum disorders. Mol Autism. 2014;5(1):19.
46. Larner O, et al. A need for consistency in behavioral phenotyping for ASD: analysis of the valproic acid model. Autism Res Treat. 2021;2021(1):8863256.
47. Stridh L, et al. Toll-like receptor-3 activation increases the vulnerability of the neonatal brain to hypoxia–ischemia. J Neurosci. 2013;33(29):12041–51.
48. Wang Y, et al. TLR4-NF-κB signal involved in depressive-like behaviors and cytokine expression of frontal cortex and hippocampus in stressed C57BL/6 and Ob/Ob mice. Neural Plast. 2018;2018(1):7254016.
49. Young AM, et al. Aberrant NF-kappaB expression in autism spectrum condition: a mechanism for neuroinflammation. Front Psychiatry. 2011;2:27.
50. Xiao L, et al. Critical role of TLR4 on the microglia activation induced by maternal LPS exposure leading to ASD-like behavior of offspring. Front Cell Dev Biol. 2021;9: 634837.
51. Zhu L, et al. Toll-like receptor 4/nuclear factor-kappa B pathway is involved in radicular pain by encouraging spinal microglia activation and inflammatory response in a rat model of lumbar disc herniation. Korean J Pain. 2021;34(1):47.
52. Gozal E, et al. Potential crosstalk between sonic hedgehog-WNT signaling and neurovascular molecules: Implications for blood–brain barrier integrity in autism spectrum disorder. J Neurochem. 2021;159(1):15–28.
53. Lamparter CL, Philbrook NA, Winn LM. Valproic acid increases NF-κB transcriptional activation despite decreasing DNA binding ability in P19 cells, which may play a role in VPA-initiated teratogenesis. Reprod Toxicol. 2017;74:32–9.
54. Karki R, Igwe OJ. Toll-like receptor 4–mediated nuclear factor kappa B activation is essential for sensing exogenous oxidants to propagate and maintain oxidative/Nitrosative cellular stress. PLoS ONE. 2013;8(9): e73840.
55. Yousefi-Manesh H, et al. Risperidone attenuates acetic acid-induced colitis in rats through inhibition of TLR4/NF-kB signaling pathway. Immunopharmacol Immunotoxicol. 2020;42(5):464–72.
56. MacDowell KS, et al. Risperidone normalizes increased inflammatory parameters and restores anti-inflammatory pathways in a model of neuroinflammation. Int J Neuropsychopharmacol. 2013;16(1):121–35.
57. Gao W, et al. Inhibition of toll-like receptor signaling as a promising therapy for inflammatory diseases: a journey from molecular to nano therapeutics. Front Physiol. 2017;8:508.
58. Bahrami A, et al. Effect of statins on toll-like receptors: a new insight to pleiotropic effects. Pharmacol Res. 2018;135:230–8.
59. Azirak S, et al. Thymoquinone prevents valproic acid-induced nephrotoxicity in rat kidney. Eurasian J Biol Chem Sci. 2022;5(2):77–84.
60. Schiavone S, et al. Involvement of NOX2 in the development of behavioral and pathologic alterations in isolated rats. Biol Psychiatry. 2009;66(4):384–92.
61. Bedard K, Krause KH. The NOX family of ROS-generating NADPH oxidases: physiology and pathophysiology. Physiol Rev. 2007;87(1):245–313.
62. Ryter SW, et al. Mechanisms of cell death in oxidative stress. Antioxid Redox Signal. 2007;9(1):49–89.
63. Rayegan S, Dehpour AR, Sharifi AM. Studying neuroprotective effect of Atorvastatin as a small molecule drug on high glucose-induced neurotoxicity in undifferentiated PC12 cells: role of NADPH oxidase. Metab Brain Dis. 2017;32:41–9.
64. Yan J, et al. Atorvastatin improves motor function, anxiety and depression by NOX2-mediated autophagy and oxidative stress in MPTP-lesioned mice. Aging. 2021;13(1):831.
65. Kim SW, et al. Statins and inflammation: new therapeutic opportunities in psychiatry. Front Psychiatry. 2019;10:103.
66. Rana SV. Metals and apoptosis: recent developments. J Trace Elem Med Biol. 2008;22(4):262–84.
67. Shalini S, et al. Old, new and emerging functions of caspases. Cell Death Differ. 2015;22(4):526–39.
68. Masliah E, et al. Caspase dependent DNA fragmentation might be associated with excitotoxicity in Alzheimer disease. J Neuropathol Exp Neurol. 1998;57(11):1041–52.
69. Hartmann A, et al. Caspase-3: a vulnerability factor and final effector in apoptotic death of dopaminergic neurons in Parkinson's disease. Proc Natl Acad Sci USA. 2000;97(6):2875–80.
70. Sheikh AM, et al. Cathepsin D and apoptosis related proteins are elevated in the brain of autistic subjects. Neuroscience. 2010;165(2):363–70.
71. Hussein AM, et al. Possible mechanisms of the neuroprotective actions of date palm fruits aqueous extracts against valproic acid-induced autism in rats. Curr Issues Mol Biol. 2023;45(2):1627–43.
72. Abekawa T, et al. Olanzapine and risperidone block a high dose of methamphetamine-induced schizophrenia-like behavioral abnormalities and accompanied apoptosis in the medial prefrontal cortex. Schizophr Res. 2008;101(1–3):84–94.
73. Bayatmakoo R, et al. Atorvastatin inhibits cholesterol-induced caspase-3 cleavage through down-regulation of p38 and up-regulation of Bcl-2 in the rat carotid artery. Cardiovasc J Afr. 2017;28(5):298–303.
74. Piermartiri TC, et al. Atorvastatin prevents hippocampal cell death, neuroinflammation and oxidative stress following amyloid-β1–40 administration in mice: Evidence for dissociation between cognitive deficits and neuronal damage. Exp Neurol. 2010;226(2):274–84.
75. Sodero AO, Barrantes FJ. Pleiotropic effects of statins on brain cells. Biochim Biophys Acta Biomembr. 2020;1862(9): 183340.
76. Lübtow MM, et al. In vitro blood-brain barrier permeability and cytotoxicity of an atorvastatin-loaded nanoformulation against glioblastoma in 2D and 3D models. Mol Pharm. 2020;17(6):1835–47.
77. Kumar H, Sharma B. Memantine ameliorates autistic behavior, biochemistry and blood brain barrier impairments in rats. Brain Res Bull. 2016;124:27–39.
78. Kim KC, et al. Male-specific alteration in excitatory post-synaptic development and social interaction in pre-natal valproic acid exposure model of autism spectrum disorder. J Neurochem. 2013;124(6):832–43.
79. Melancia F, et al. Sex-specific autistic endophenotypes induced by prenatal exposure to valproic acid involve anandamide signalling. Br J Pharmacol. 2018;175(18):3699–712.
80. Varadinova M, Bogdanov G, Markova P. Effects of risperidone on learning and memory parameters in experimental model of autism. Trakia J Sci. 2019;17(3):203.
81. Boman L, De Butte M. Neurobehavioral effects of chronic low-dose risperidone administration in juvenile male rats. Behav Brain Res. 2019;363:155–60.
82. Abd Elazeem AH, et al. The ameliorative effect of apigenin or silymarin as add-on therapy to risperidone on valproic acid induced autism in albino rats: implication of oxidative stress, apoptosis and autophagy. Egypt J Hosp Med. 2023;90(1):1245–55.
83. Kalonia H, Kumar P, Kumar A. Comparative neuroprotective profile of statins in quinolinic acid induced neurotoxicity in rats. Behav Brain Res. 2011;216(1):220–8.
84. Saito T, et al. Continuous oral administration of atorvastatin ameliorates brain damage after transient focal ischemia in rats. Life Sci. 2014;94(2):106–14.

85. Cho H, et al. Changes in brain metabolic connectivity underlie autistic-like social deficits in a rat model of autism spectrum disorder. Sci Rep. 2017;7(1):13213.
86. Castelhano-Carlos M, et al. PhenoWorld: a new paradigm to screen rodent behavior. Transl Psychiatry. 2014;4(6): e399.
87. Motaghinejad M, et al. Topiramate via NMDA, AMPA/kainate, GABA(A) and Alpha2 receptors and by modulation of CREB/BDNF and Akt/GSK3 signaling pathway exerts neuroprotective effects against methylphenidate-induced neurotoxicity in rats. J Neural Transm (Vienna). 2017;124(11):1369–87.
88. Feizipour S, et al. Selegiline acts as neuroprotective agent against methamphetamine-prompted mood and cognitive related behavior and neurotoxicity in rats: involvement of CREB/BDNF and Akt/GSK3 signal pathways. Iran J Basic Med Sci. 2020;23(5):606.
89. Ghafarimoghadam M, et al. A review of behavioral methods for the evaluation of cognitive performance in animal models: current techniques and links to human cognition. Physiol Behav. 2022;244: 113652.
90. Kamel MM, El-lethey HS. The potential health hazard of tartrazine and levels of hyperactivity, anxiety-like symptoms, depression and anti-social behaviour in rats. J Am Sci. 2011;7(6):1211–8.
91. Magdy A, et al. Neuroprotective and therapeutic effects of calcitriol in rotenone-induced Parkinson's disease rat model. Front Cell Neurosci. 2022;16: 967813.
92. Florell SR, et al. Preservation of RNA for functional genomic studies: a multidisciplinary tumor bank protocol. Mod Pathol. 2001;14(2):116–28.
93. Xu Q, et al. Abnormal development pattern of the amygdala and hippocampus from childhood to adulthood with autism. J Clin Neurosci. 2020;78:327–32.
94. Banker SM, et al. Hippocampal contributions to social and cognitive deficits in autism spectrum disorder. Trends Neurosci. 2021;44(10):793–807.
95. Chomczynski P. A reagent for the single-step simultaneous isolation of RNA, DNA and proteins from cell and tissue samples. Biotechniques. 1993;15(3):532–4, 536-7.
96. Freeman WM, Walker SJ, Vrana KE. Quantitative RT-PCR: pitfalls and potential. Biotechniques. 1999;26(1):112–22.
97. Livak KJ, Schmittgen TD. Analysis of relative gene expression data using real-time quantitative PCR and the $2^{-\Delta\Delta CT}$ method. Methods. 2001;25(4):402–8.
98. Bancroft JD, Layton C. The hematoxylins and eosin. Bancroft's Theory Pract Histol Techn. 2012;7:173–86.
99. Jackson P, Blythe D. Immunohistochemical techniques. Theory Pract Histol Techn. 2008;7:381–426.

Publisher's Note